Carbothermic Reduction of Bauxite Residue for Iron Recovery and Subsequent Aluminium Recovery from Slag Leaching

Pritii Tam Wai Yin[1], Buhle Xakalashe[2], Bernd Friedrich[3], Dimitrios Panias[4] and Vicky Vassiliadou[5]
1. PhD Candidate
Aluminium of Greece, Agios Nikolaos, Viotia, Greece
2. PhD Candidate
3. Professor
RWTH Aachen, IME Institute of Process Metallurgy and Metal Recycling, Aachen, Germany
4. Professor
National Technical University of Athens, School of Mining and Metallurgical Engineering, Athens, Greece
5. Head of Continuous Improvement and Systems Management
Aluminium of Greece, Agios Nikolaos, Viotia, Greece
Corresponding author: pritii.tam@metal.ntua.gr

Abstract

Industrially and historically, alternative processes were developed to recover alumina from low-grade ores of non-bauxitic origin as well as for economic reasons. The Pedersen process from Norway was adapted towards high ferruginous and high silica containing bauxitic ores. This paper considers the adaptation of the Pedersen pyro-hydrometallurgical route of reductive smelting with lime and coke to recover iron and aluminium from bauxite residue (BR), which is the by-product of the Bayer process where aluminium is typically lost in complex desilication product matrices. Greek BR was firstly smelted in an Electric Arc Furnace (EAF) to recover pig iron (>95 %). The fluxing strategy entailed feeding lime to favour lower operating temperatures (1500–1550 °C) and slag viscosities, and to produce a slag containing calcium aluminate phases ($12CaO\cdot7Al_2O_3$, $3CaO\cdot Al_2O_3$ and $CaO.Al_2O_3$). The calcium aluminates were identified as thermodynamically favourable in descending order to form $NaAlO_2$ when leached in Na_2CO_3 solution (ΔG_{rxn}^{298K}= -782, -188 and -68 kJ/mol, respectively). Leaching temperature, Na_2CO_3 concentrations, residence time and different particle sizes were varied to investigate the leachability of slags for aluminium recovery; up to 43 % aluminium was recovered with 95 % of silicon content remaining in leached residue. SEM studies also aided understanding of interstitial leaching mechanism.

Keywords: Bauxite residue, electric arc furnace, pig iron recovery, calcium aluminate, aluminium recovery.

1. Introduction

The recovery of aluminium became a favourable production option largely because of the discovery of bauxitic ore that contained high aluminium-bearing components such as gibbsite (γ-$Al(OH)_3$), boehmite (γ-AlO(OH)) and diaspore (α-AlO(OH)). Hydrometallurgical Bayer processing has invariably outcompeted pyrometallurgical routes because of its economic viability in extracting alumina from high and several medium grade ores. However, the scarcity of bauxitic ores during and right after World War II became a crux of research initiatives that was driven to investigate alternative viable methods of production using lower-grade ores [1, 2]. One such method was the practice of a pyrometallurgical-based Pedersen process in Norway. The original Pedersen process focused on the smelting of bauxite, iron ore, lime and coke to recover low-silica calcium aluminate slag and metallic iron, followed with leaching of slag with sodium carbonate solution to achieve the formation and dissolution of sodium aluminate [2].

The plant in Høyanger, Norway (1928-1969) had an annual production of around 17,000 metric tons [3]. Hignett et al [2] reiterated the process in 1942 using clay as a raw aluminium source instead, in both laboratory scale and pilot plant level. The process was also adapted by Blake et al [3] during 1966 towards high-silica and titania bauxites of Pacific Northwest (U.S.A). Fly ashes were also proposed to be adapted towards the lime-sinter process [4]. In the past literature, it is important to note that lime-sinter process and smelting process are often used interchangeably as the formation of desirable calcium aluminates operate close to its eutectic point.

Miller and Irgens [1] sourced the bauxite from Greece, containing a high percentage of boehmite (58.5 wt% Al_2O_3). After the addition of limestone and coke, the molten slag was smelted continuously at 1500 °C, where it was tapped every 6 hours for pig iron and calcium aluminate slag. The slag was then cooled for four hours before crushing and leaching. 5 metric tons of slag added to 200 m^3 of lye (15 gpl total alkaline). The first leaching step was completed after 5 ½ hours at 40 °C until the lye reaches 13-14 gpl Al_2O. The mixture was then emptied into a clarifier, where underflow was treated in the second leaching step. Saturated liquor was next sent to the precipitation section.

Using clay and limestone as the raw materials, Hignett et al [2] achieved about 90 to 95 % of “soluble” alumina content from total alumina in slag (operational temperature range: 1360-1400 °C). Laboratory-scale results showed maximum extractions was achieved in the temperature range of 45 °C to 65 °C, residence time of 15 to 30 min, and > 1.6 moles Na_2CO_3 per mole of alumina (20 g sinters/200 mL of 3 % sodium carbonate). Higher silica (Si) content of the raw material was found to influence co-leaching of Si element into leachate.

The use of ferruginous bauxites by Blake et al [3] was divided into two samples in the research investigation, high silica and low silica bauxites (13.5 and 4.5 wt% SiO_2 respectively). Extra lime was added in the system to promote the formation of perovskite ($CaTiO_3$). Samples were then smelted at 1750 °C and the slag was left to cool slowly in the furnace overnight. Both sample types were tested in a range of leaching time and temperatures while keeping Na_2CO_3 concentration and solid-to-liquid ratio constant (15 g slag/ 250 mL liquor at 11 gpl Na_2CO_3 concentration). Alumina from high silica slag was best leached for 16 hours at 25 °C (70 % Al_2O_3 extraction), whereas low silica slag achieved maximum leachability (88 % Al_2O_3 extraction) at the same temperature in 8-10 hours.

Bauxite residue contains typically 13-25 % of alumina content from Bayer processing. Silica is a very important impurity that affects alumina product quality and causes chemical soda losses due to the formation of desilication products (DSP) such as Bayer cancrinites and hydrogrossular phases [5]. DSP also builds up in scales in evaporators, retarding the heat transfer. Currently, bauxite residue estimates are ever increasing with 150 million tonnes produced per annum globally [6]. Current research initiatives are focused on exploring bauxite residue as a part of a zero-waste approach. Being the host of leftover products and complex matrices, enriched bauxite residue contains a considerable amount of value in the form of titanium containing compounds and rare earths.

The main incentive for smelting bauxite residue is to recover iron, however, iron recovery on its own is not sufficient to justify the smelting of bauxite residue since bauxite residue is an inferior source of iron compared to primary iron ores. Current researches on bauxite residue smelting is experiencing a shift towards complete valorisation of bauxite residue, such as Balomenos et al [7] that conducted semi-industrial scale tests on the recovery of pig iron and viscous slag using an Electric Arc Furnace operating at 1540 °C. The slag was subsequently transformed into mineral wool. Borra et al [8] recovered pig iron at 1500-1600 °C, with the aim to enrich leftover slag for acid leaching of rare earths downstream. In another work, Borra et al [9] also removed about 66 % of aluminium (Al) from soda sintering and leaching, followed by smelting with 97 % of iron recovery, leaving the slag residue open to rare earths processing downstream.

Following the previous works towards bauxite residue, Kaußen and Friedrich [10] looked into the recovery of aluminium via three different methods; a) Bayer-type process, b) Bayer-type process with slag leaching, and c) soda sinter process. The term 'Bayer-type' is used to allude to high pressure-temperature leaching of bauxite residue done in stages, beginning with 150 min leaching of untreated bauxite residue at 270-280 °C (7 g material/30 ml), and then increasing solid-to-liquid ratio (140g material/850 mL) to either 170, 200 or 250 °C for 120 min. Aluminium was recovered up to 72 % with addition of calcium under Ca/Si ratio of 2.5, 120 min leaching and 200 gpl NaOH concentration. Method (b) used enriched slag after the removal of pig iron from smelting of bauxite residue with lignite coke and lime. The following Bayer-type procedure noticeably underperformed at 200 gpl NaOH concentrations (50 % Al recovery), and when pushed to 500 gpl NaOH and at temperatures to above 250 °C, aluminium recoveries are >90 % as the calcium aluminate and calcium aluminium silicate bonds are broken. Undissolved calcium aluminate (as $3CaO·Al_2O_3$ and $4CaO·3Al_2O_3$), gehlenite ($2CaO·Al_2O_3·SiO_2$) and grossular products remained in the leached residue.

This paper will focus on mayenite ($12CaO·7Al_2O_3$), tricalcium aluminate ($3CaO·Al_2O_3$) and monocalcium aluminate ($CaO·Al_2O_3$) production during slag enrichment as iron is recovered to the metallic product. Low temperature Na_2CO_3 leaching is performed to recover Al.

1.1. Slag Conditioning

Reaction (1) and (2) indicate general reactions to form metallic iron and calcium aluminate products during the smelting process.

$$Fe_2O_3 + 3C = 2Fe + 3CO \tag{1}$$
$$xCaO + yAl_2O_3 = xCaO·yAl_2O_3 \tag{2}$$

The reductant addition is chiefly dependent on Equation 1 with CO forming at high temperatures via Boudouard reaction. The reduction of iron is accompanied by the reduction of other oxides varying in strength from minor reduction of ignoble oxides such as SiO_2 to near complete reduction of NiO. Conditions of smelted slag and pig iron in Table 1 are described in Section 2 (Materials and Methodology).

It is clear that slag conditioning to favour the formation of desired calcium aluminate species is crucial towards leaching and recovery of aluminium. Miller and Irgens [1] also stated that the suitable slag is formed in a fairly restricted area towards monocalcium aluminate. Under slow cooling conditions, the formation of the composite mayenite species is favoured. They also warned of the issue of this narrow range that forms an unwanted tertiary insoluble gehlenite product, which can be resolved by increasing lime content (Figure 1). With the presence of titanium and silica in bauxite residue, the additional lime content will also ensure titanium is tied as perovskite and silica as dicalcium silicate. Slow cooling will also help promote the phase change of dicalcium silicate from beta to its gamma form, producing a self-disintegrating slag as it expands during this second order phase transition [4].

Lu et al [11] and Wang et al [12] both described the affinity of MgO in the $CaO-Al_2O_3-SiO_2$ slag if higher than 3 % by forming calcium aluminate magnesium silicate species that may necessitate Na_2O addition. However, since the employed Greek bauxite residue contains less than 0.3 % of MgO, it was not needed. Table 1 shows chemical analysis of bauxite residue, enriched slag and pig iron via XRF. Bauxite residue of this research was obtained from Aluminium of Greece located in Boeotia, Greece.

Table 1. Chemical composition (by XRF) of AoG bauxite residue and of materials after smelting.

Component (wt%)	**Na_2O**	**Al_2O_3**	**CaO**	**SiO_2**	**V_2O_5**	**TiO_2**	**Fe_2O_3**	**P_2O_5**	**LOI**
AoG bauxite residue	1.97	25.28	8.49	6.23	0.19	5.02	44.28	0.13	9.53
Smelted Slag	0.54	31.5	53.9	8.87	0.08	6.19	0.64	0.04	-0.86
Pig Iron			**C**	**Si**	**V**	**Ti**	**Fe**	**P**	**S**
			5.1	0.1	0.2	0.3	93	0.2	0.006

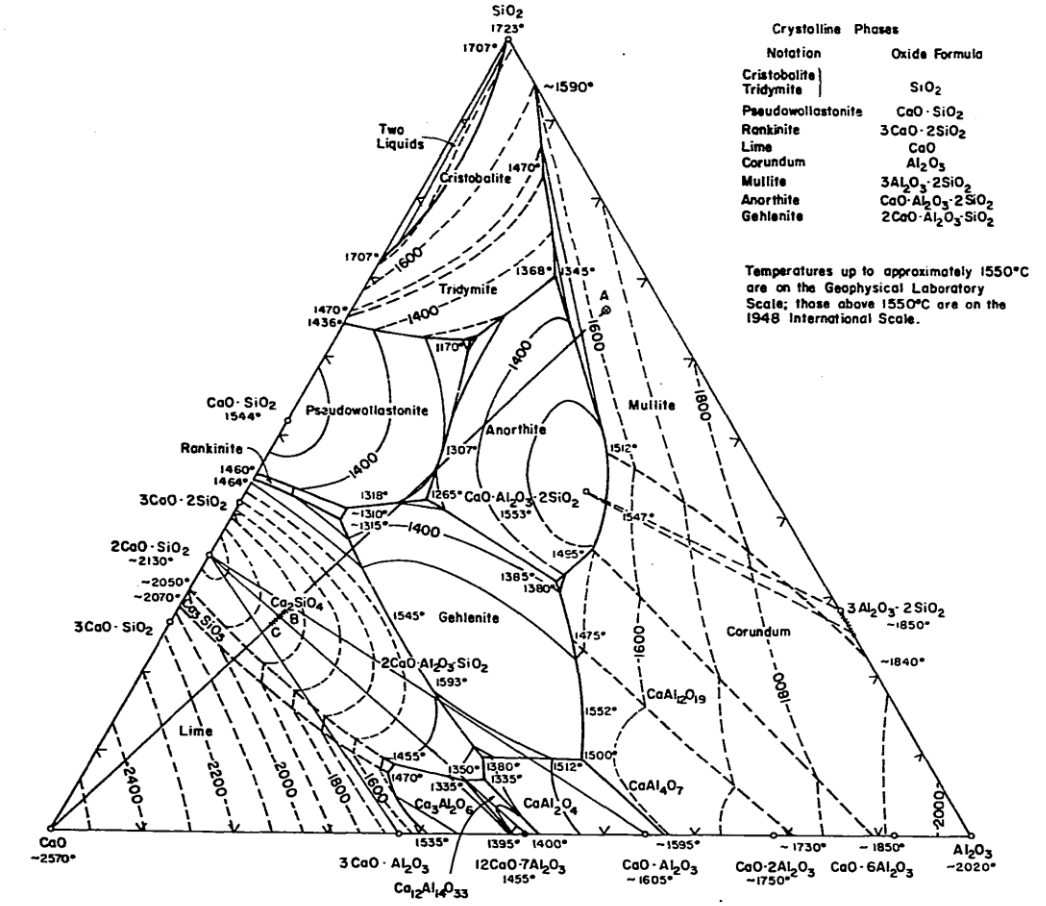

Figure 1. Phase diagram of $CaO-Al_2O_3-SiO_2$ [4, 13].

Chou and Burnet [4] proposed an overall mechanism based on a kinetic study of pure $CaO-Al_2O_3-SiO_2$ system with regards to the formation of calcium aluminates. From their studies, they noted that the mechanism of formation of calcium aluminate leading to mayenite's eutectic point at 1455 °C. $12CaO·Al_2O_3$ is the predicted primary product with $CaO·Al_2O_3$ becoming the first dominant phase as alumina particles are converted. $3CaO·Al_2O_3$ exists as an intermediate phase as calcium ions continually diffuse into the primary particle. As CaO becomes totally consumed, $12CaO·Al_2O_3$ appears again from $3CaO·Al_2O_3$ and $CaO·Al_2O_3$ consumption.

1.2. Na_2CO_3 Leaching of Slag

Low temperature treatment was chosen as the preferred leaching method for this study as pure mayenite species is notably leached up to 92 % by Sun et al [14] in temperature of 75 °C, leaching time of 30 min, solid-to-liquid ratio of 1:10 and leaching concentrations of 120 gpl Na_2CO_3 and 7 gpl free NaOH. The target leachable phases are given in equation (3) to (5). Unwanted side reaction occurs as equation (6).

$$CaO \cdot Al_2O_3 + Na_2CO_3 = Na_2O \cdot Al_2O_3 + CaCO_3 \quad (3)$$

$$3CaO \cdot Al_2O_3 + 3Na_2CO3 = 3Na_2O \cdot Al_2O_3 + 3CaCO_3 \quad (4)$$

$$12CaO \cdot 7Al_2O_3 + 12Na_2CO_3 + 5H_2O = 7Na_2O \cdot Al_2O_3 + 12CaCO_3 + 10NaOH \quad (5)$$

$$2CaO \cdot SiO_2 + 2Na_2CO_3 + H_2O = Na_2O \cdot SiO_2 + 2CaCO_3 + 2NaOH \quad (6)$$

From Factsage software [15] and HSC software [16], the thermodynamic heat and Gibbs energy of reaction is predicted in the given Table 2 below, assuming reaction of calcium aluminate with NaOH component formed from the complete dissolution of Na_2CO_3 species in water. Mayenite species in Factsage is assumed to be $Ca_{12}Al_{14}F_2O_{32}$ as the form of the mineral that is available in the database. Despite a larger amount of difference of the values for heat and gibbs energy of mayenite species between Factsage and HSC software, the Gibbs energy and spontaneity of reaction is at least 4 times higher than the subsequent tricalcium aluminate species, reinforcing that mayenite is a more suitable leachable species. Though Gibbs energy values are competitive for both $CaO \cdot 2Al_2O_3$ and $CaO \cdot 6Al_2O_3$ against $3CaO \cdot Al_2O_3$ species, the two former species are formed at a much higher smelting temperature of 1700 °C and above (Figure 1). The heat of reaction released is also proportionally higher for mayenite species, indicating mayenite species favouring forward reaction during leaching at low temperatures and hindered at higher temperatures.

Table 2. Thermodynamic heat and Gibbs energy of reaction of calcium aluminates with caustic leaching at 25 °C (Factsage™ Software [15], HSC™ Software [16]).

Species	**Factsage™**		**HSC™**	
(kJ/mol reactant)	ΔG_{rxn}^{298K}	ΔH_{rxn}^{298K}	ΔG_{rxn}^{298K}	ΔH_{rxn}^{298K}
$3CaO \cdot Al_2O_3$	-189.40	-213.04	-188.10	-213.04
$CaO \cdot Al_2O_3$	-70.55	-76.45	-68.77	-74.40
$CaO \cdot 2Al_2O_3$	-101.06	-101.26	-102.09	-102.26
$CaO \cdot 6Al_2O_3$	-232.05	-198.16	-240.51	-210.28
$12CaO \cdot 7Al_2O_3$*	-682.62	-764.46	-782.17	-875.25

*Mayenite species in Factsage exists as $Ca_{12}Al_{14}F_2O_{32}$

2. Materials and Methodology

The bauxite residue received from AoG was dried at 105 °C for 24 hours to remove surface moisture. 1.5 kg of dried sample was mixed with 600 g lime (40 % addition, commercial purity 95 wt% CaO) as a fluxing agent, and lignite coke (87 % C) at 10 % addition. The prepared material was fed into a 100 KVA DC electric arc furnace operated at about 5 kW and smelted batch wise in a graphite crucible at 1500 – 1550 °C for an hour. The molten material was then tapped into a refractory lined mould where the material solidified into distinct slag and metal phases. The slag and metal were subsequently separated and weighed.

The slag was crushed and milled, and finally sieved to obtain slag particle size of between 90 µm and 125 µm. Chemical analysis of the different size fractions were also performed to ensure the sample was homogenous. Sample of particle size below 90 µm was retained to compare the influence of particle size during leaching. Table 3 shows the chemical analysis of the milled slag of different particle sizes, indicating homogeneity of the formed slag.

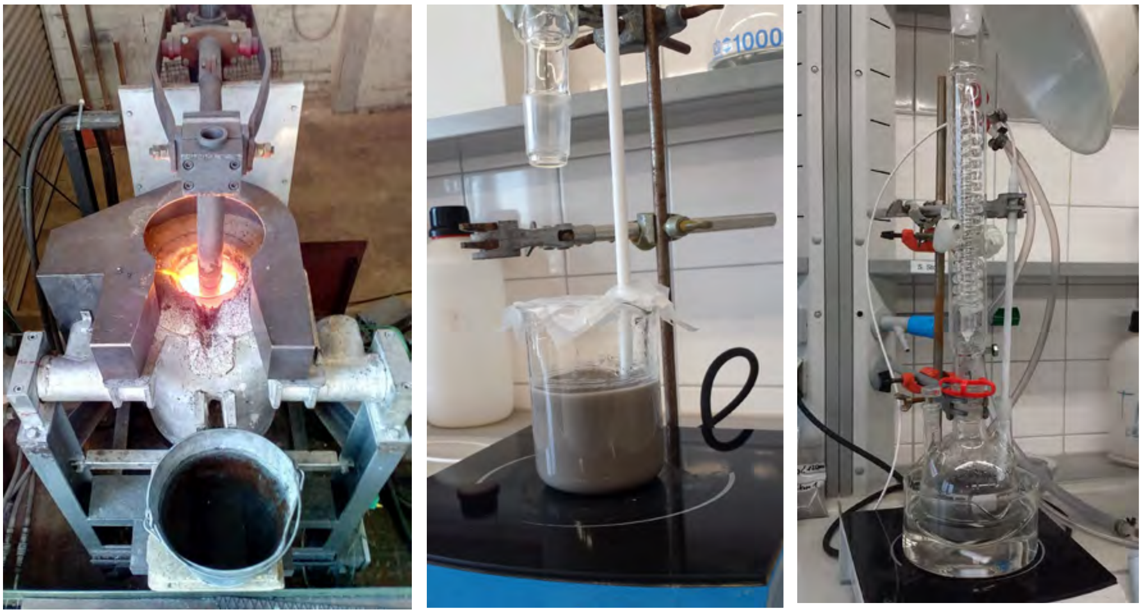

Figure 2. Experimental set-up (from left to right), Electric Arc Furnace, Leaching reactor A, Leaching reactor B.

Table 3: Chemical analysis of the milled and sieved slag (XRF).

Components (wt%)	Na_2O	Al_2O_3	CaO	SiO_2	V_2O_5	TiO_2	Fe_2O_3
$x < 90$ µm	0.14	31.7	57.6	8.92	0.047	5.87	0.45
$90<x<125$ µm	0.13	31.4	57.0	8.89	0.042	5.81	0.54
>125 µm	0.1	31.3	57.0	8.89	0.041	5.77	0.51

The Na_2CO_3 leaching of slag focused on low temperature treatment, varying leaching conditions as follows: temperatures (40, 60, 80, 90 °C), sodium carbonate concentrations (50, 100, 150, 300 gpl Na_2CO_3, anhydrous powder 99.5 %) and residence times (15 min, 30 min, 1 hour and 4 hours). Figure 2 shows the designed experimental set-up detailing the reactors used for the leaching experiments. Leaching experiments at 40 and 60 °C were carried out in reactor A, assuming negligible evaporative losses while leaching experiments at 80°C and 90°C were carried out in reactor B, to prevent evaporative losses at higher temperatures. Solid-to-liquid ratio was kept constant (25 g slag/ 250 mL of liquor). Both leaching reactors were designed to operate continuously for the duration of 4 hours, 6 mL sampling was done with a glass pipette, filtered and diluted for ICP-OES analysis.

2.1. Chemical and Mineralogical Analysis

The samples of slag and leach residues were analysed by XRF glass disc (model: PANanlytical Axios) with lithium tetraborate flux and XRD (model: BruckerD8 with Cu-Kα1-radiation 1.5407 A° ,40 kV, 40 mA). Leachates were analysed using inductively coupled plasma optical emission spectrometry (ICP-OES, model: Spectro ICP-OES Spectro Flame D). SEM preparation of the slag and leached residue involved dry samples independently or embedded in epoxy resin, polished and cross-section coated with carbon. SEM images were performed on Jeol6380V Scanning Electron Microscope with energy-dispersive X-ray spectroscopy (SEM/EDS) under back-scattering mode and secondary electron image mode (Accelerating voltage: 15-20 kV, Filament heating: 80-82 µt, Low vacuum control: 30 Pa). Renishaw inVia Raman microscope used laser power of 532 nm. Pig iron bulk analysis was done using spark spectrometers and LECO for C and S analysis.

3. Results and Discussion

The low residual iron in slag as presented in Table 1 accompanied by good slag metal separation was in agreement with high iron recoveries reported at 95 % during the smelting process. The slag shows a low Na_2O content which was attributed to the reduction of this oxide in the highly basic slag and a subsequent evaporation of metallic Na (g). The combination of the highly reducing conditions in the furnace accompanied by high CaO content proved favourable for desulfurization. The mineralogy of produced slag was evaluated relative to the starting bauxite residue and of final leached residue for a combined Fe and Al recovery in Figure 3.

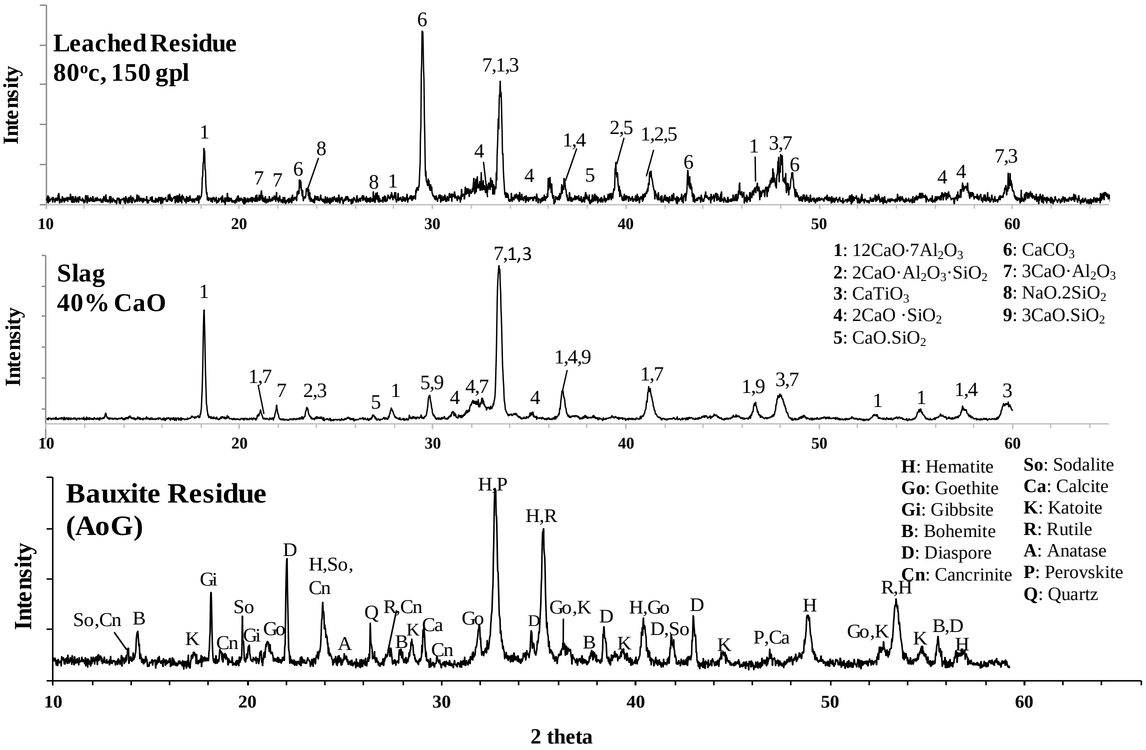

Figure 3. XRD of Bauxite Residue, Slag Phase from EAF smelting, and Leached Residue.

Interpreting the XRD figure of the slag and leached residue was difficult as the characteristic peaks of calcium aluminate species are closely related to each other. As a guideline, $12CaO{\cdot}7Al_2O_3$ appears at 2 theta values of 33.4°, 18.14° and 36.7°, in the order of decreasing intensity. Followed by $CaO{\cdot}Al_2O_3$ at 30.1°, 35.6° and 37.3° and finally, $3CaO{\cdot}Al_2O_3$ at 33.2°, 47.7° and 59.3°. It was clear from the initial XRD of the slag from 40 % CaO addition that the aluminium-bearing species from bauxite residue has been completely broken down and transformed into mayenite, minor gehlenite and tricalcium aluminate.

The presence of excess Ca in the form of calcite (6) was strongly detected after leaching which confirms forward reactions of equations (3-6). However, XRD transformation after leaching was shown not to dissolve mayenite species completely (Peak 1). The intensity of mayenite peak was roughly halved after leaching, and since leachate recoveries from Figure 5 (a-e) are around 40 %-50 % levels. and it is plausible that aluminium recovery stems from the partial leaching of mayenite species in the liquor. Perovskite main characteristic peak (XRD peaks 33.2°,47.6° and 59.3° in decreasing intensity) coincides with mayenite and tricalcium aluminate peaks, making it difficult to identify the proportions of calcium aluminates present, though since Peak 1 is mainly attributed to mayenite, mayenite species leaching requires a more concentrated effort in ensuring the appropriate leachable crystalline phases are formed during cooling of slag.

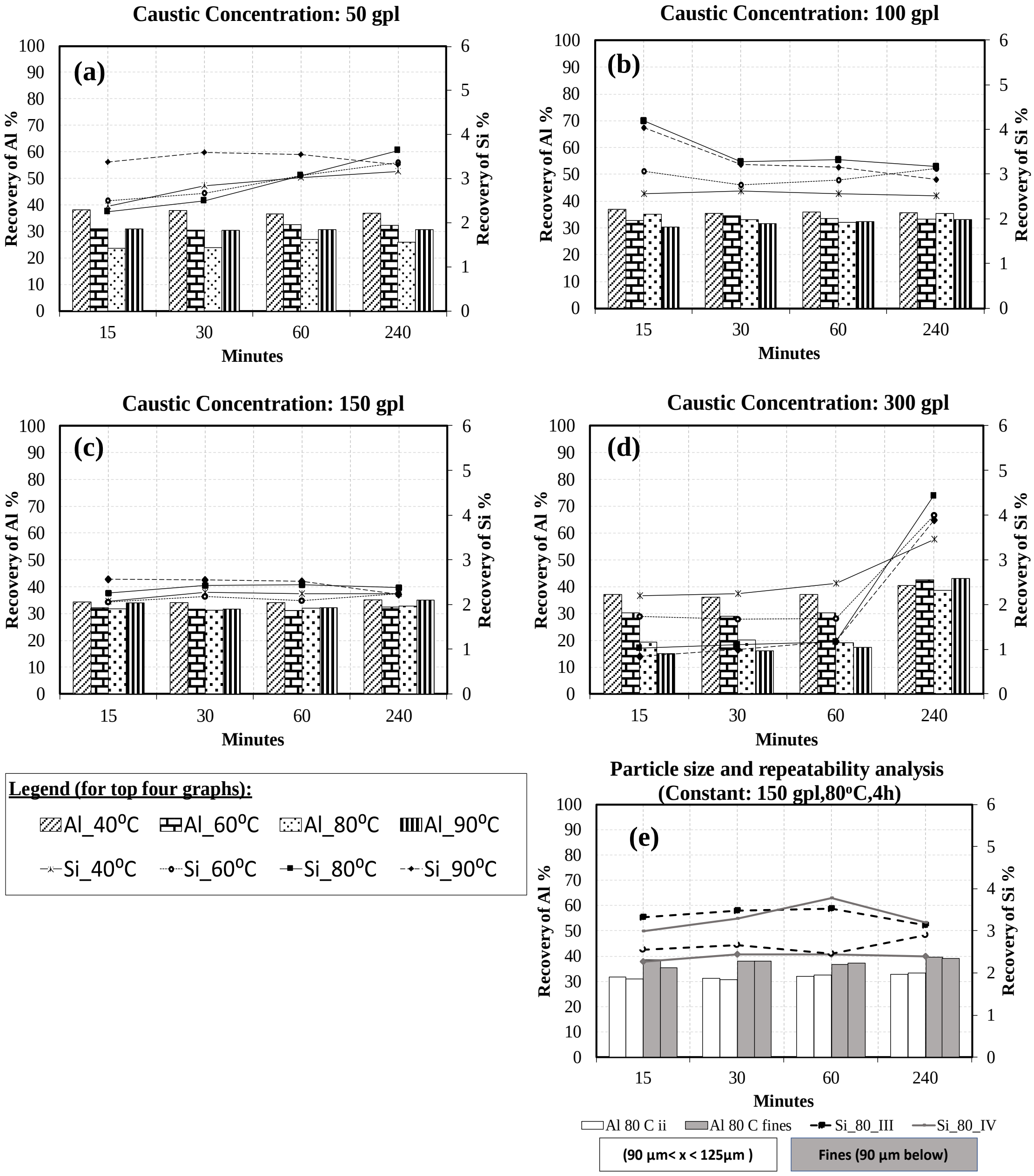

Figure 4. Al (left axes) and Si (right axes) recoveries from leachate (ICP-OES) in wt%.

From Figure 4, the achieved leaching recoveries are less than 50 % in this current stage of research, though it was interesting to note that thermodynamic data (Table 3) agrees with experimental results where it was exothermic when in contact with Na_2CO_3 solution. This shows in the results where 40 °C leaching temperature reaches a higher amount of aluminium recovery, and that the exothermic nature of reaction was inhibited at higher leaching temperatures.

The differences of temperature choice are a lot more apparent in higher Na_2CO_3 concentration levels, where recoveries of Al are less than 20 % in the initial 15 min, 30 min and 60 min residence time for 300 gpl Na_2CO_3 (d). After 4 hours of leaching, aluminium leaching appears to reach saturation for 100 gpl Na_2CO_3 levels and above. Si levels are within 2-4 %, with 150 gpl (c) hitting lowest concentrations. At higher Na_2CO_3 concentrations (d), once again Si was drawn out noticeably after 4 hours of leaching. This agrees well with past researches that spoke of the interaction of sodium silicate with sodium aluminate in liquor for longer residence time.

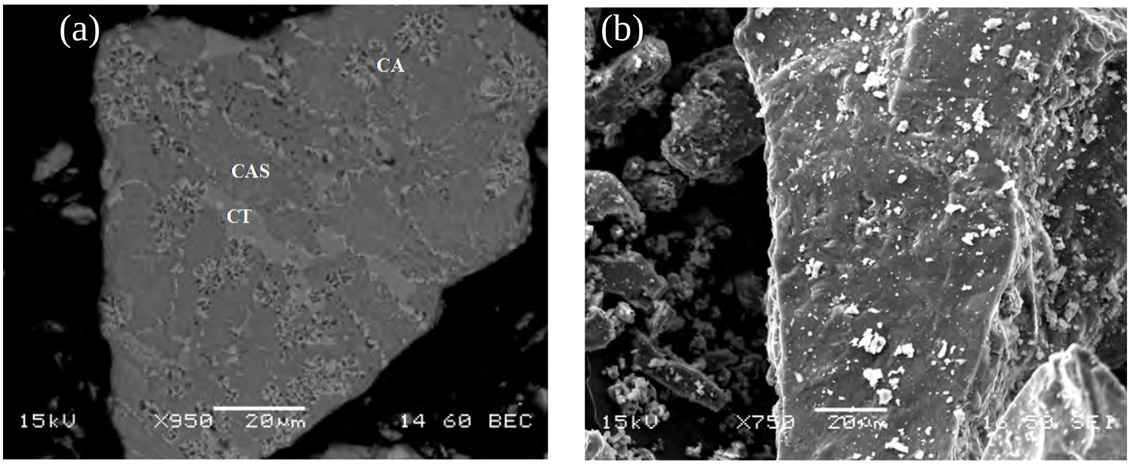

Figure 5. (a) Slag particle with major phases: calcium titanate (CT), calcium aluminium silicate (CAS), calcium aluminate (CA); (b) Topographical view of slag particle.

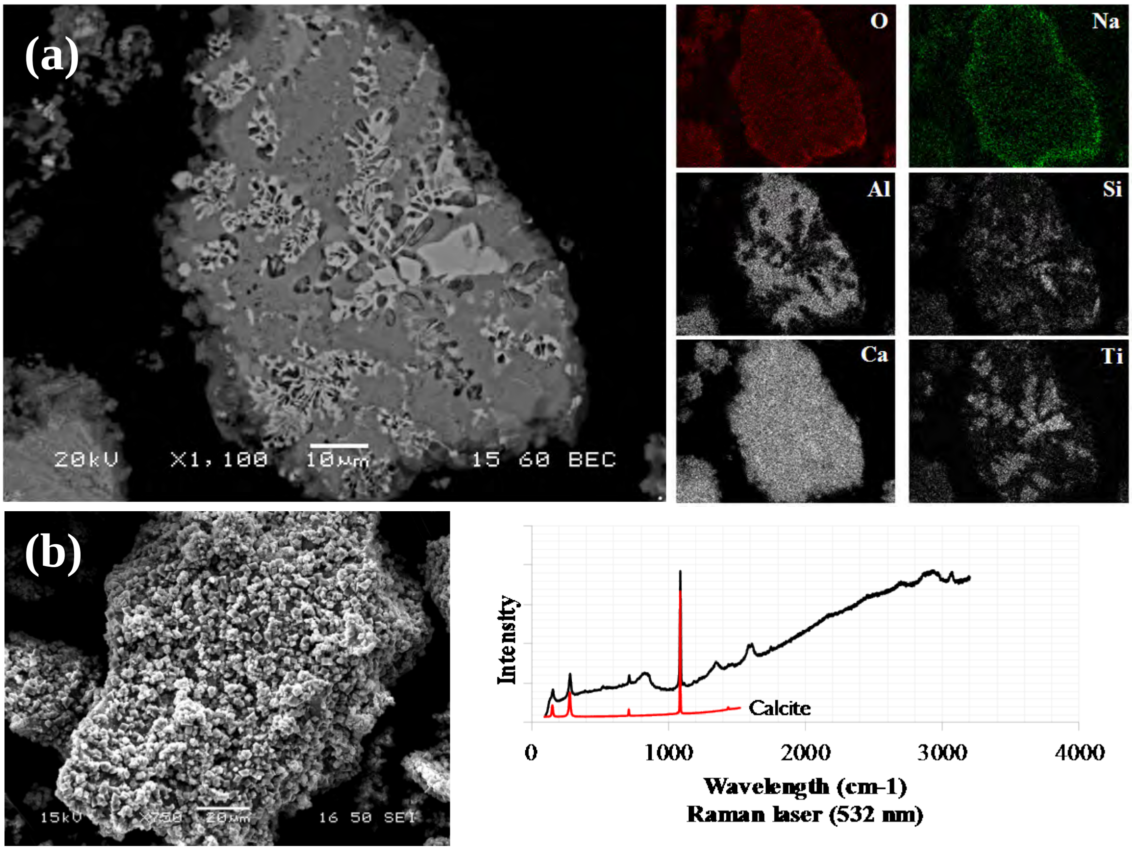

Figure 6. (a) Leached residue particle with SEM elemental mapping; (b) Topographical view and Raman confirmation of calcite.

Figure 5 above shows the SEM imaging of slag cross-section and topographical view. Calcium titanate is observed to be present in large amounts with dendritic structures forming after slag was cooled. The topographical surface of the slag was seen to be clear and smooth before leaching. SEM imaging (Figure 6, a) of the leached residue particle shows a deposition on the surface of the slag particle, and in Figure 6 (b), the topographical view and confirmation of the

Raman data indicate that calcite was deposited on the surface of the slag. SEM elemental mapping also indicates Na was found in higher levels at the surface of the slag. Again, in the Figure 4 (e) previously, it was noted that finer particle sizes of below 90 μm show slight improvement in Al recovery compared to particle sizes of 90 μm to 125 μm. All observations indicate that the leaching of the slag is surface driven. An insoluble layer of calcite build-up inhibits the dissolution of alumina from calcium aluminates in the core particle. We can also hypothesise that because of mayenite leaching that is surface driven on the slag particle, complete leaching of Al species is diffusion dependent that may require higher residence time in Na_2CO_3 solution at low temperatures.

4. Conclusion

The combined recovery of iron and aluminium from bauxite residue through the adaptation of the Pedersen process has been demonstrated successfully for the former and to be focus on improvements on the latter. The smelting of bauxite residue was undertaken at 1500 °C using lignite coke as reductant under lime fluxing, achieving high iron recoveries. The combination of highly reducing conditions during smelting and high CaO slag (54 wt% CaO) favoured desulfurization of the pig iron product. Furthermore, low sodium content was reported in the slag. The aluminium was mainly found in the mayenite and tricalcium aluminate minerals in the slag. It is recommended that the presence of these species is best confirmed through a combination effort of XRD, SEM Quantitative analysis and Raman spectroscopy.

Low aluminium recoveries were achieved for the slag leaching testwork. This is in contradiction with reported Al recoveries for calcium aluminate slags, as these slags are reported to be readily leachable under low temperature Na_2CO_3 leaching. Leaching of calcium aluminates are best done at low temperatures of below 40 °C as they are exothermic in nature. In terms of Na_2CO_3 concentration of low temperature leaching, the preferred concentrations lean towards 150 gpl Na_2CO_3 and below as higher concentration has the tendency to draw out silica into leachate. The cooling rate of slag influences the crystallization path and the formation of leachable calcium aluminate minerals and should be investigated in the future work. Leaching of calcium aluminate slag is surface driven and once again, the correct leachable crystallinity of mayenite mineral phase formation during cooling of smelting process is crucial to allow better aluminium recoveries.

5. Acknowledgement

The research leading to these results has received funding from the European Community’s Horizon 2020 Programme (H2020/2014–2019) under Grant Agreement no. 636876 (MSCA-ETN REDMUD). This publication reflects only the authors’ views, exempting the Community from any liability. Project website: http://www.etn.redmud.org.

6. References

1. Jan Miller and Aake Irgens, Alumina production by the Pedersen process: history and future, *in Essential Readings in Light Metals* 2013, John Wiley & Sons, Inc., 975-982.
2. T. P. Hignett, Pilot plants: production of alumina from clay by a modified Pedersen process. *Industrial & Engineering Chemistry,* Vol. 39, No. 8, (1947), 1052-1060.
3. Henry E. Blake, et al., Adaptation of the Pedersen process to the ferruginous bauxites of the pacific northwest. *Report of investigations / United States Department of the Interior, Bureau of Mines ;6939* Washington, D.C., 1967, U.S. Dept. of the Interior, Bureau of Mines.
4. Kan-Sen Chou, Formation of calcium aluminates in the lime-sinter process part II. Kinetic study. *Cement and Concrete Research,* Vol. 11, Vol. 2, (1981), 167-174.

5. Peter Smith, Reactions of lime under high temperature Bayer digestion conditions. *Hydrometallurgy*, Vol. 170, (2017), 16-23.
6. Ken Evans, The history, challenges, and new developments in the management and use of bauxite residue. *Journal of Sustainable Metallurgy*, (2016), 1-16.
7. Efthymios Balomenos, et al., EAF Treatment for the efficient and complete exploitation of the bauxite residue (red mud) produced in the Bayer Process, in Proceedings of the European Metallurgical Conference (EMC 2013) 2013, Weimar, Germany, 285-292.
8. Chenna Rao Borra, et al., Smelting of bauxite residue (red mud) in view of iron and selective rare earths recovery. *Journal of Sustainable Metallurgy,* Vol. 2, No. 1, (2016), 28-37.
9. Chenna Rao Borra, et al., Leaching of rare earths from bauxite residue (red mud). *Minerals Engineering,* Vol. 76, (2015), 20-27.
10. Frank M. Kaußen and Bernd Friedrich, Methods for alkaline recovery of aluminum from bauxite residue. *Journal of Sustainable Metallurgy*, (2016), 1-12.
11. Long Lu, et al., Thermodynamic analysis and formation law of Q phase of calcium aluminate clinker, *in Light Metals* 2017, Springer International Publishing, Cham, 31-35.
12. Bo Wang, et al., Effect of Na_2O on alumina leaching property and phase transformation of MgO-containing calcium aluminate slags. *Transactions of Nonferrous Metals Society of China*, Vol. 21, No. 12, (2011), 2752-2757.
13. M.I. Gasik and N.P. Liakishev, Chapter 5: Electrometallurgy ferrosilicon :The technology of smelting and casting of ferrosilicon, in Theory and technology of electrometallurgy ferroalloys: Textbook for universities in the specialty "Metallurgy of ferrous metals and alloys". In Russian: Теория и технология электрометаллургии ферросплавов : Учеб. для студентов вузов, обучающихся по специальности "Металлургия черных металлов и сплавов", *SP Intermet Engineering* 1999, Moscow, Russia.
14. Hui-lan Sun, et al., Characterization and alumina leachability of $12CaO{\cdot}7Al_2O_3$ with different holding times, in Advances in Materials Science and Engineering 2014, 6.
15. C.W. Bale, et al., FactSage thermochemical software and databases, 2010–2016. *Calphad*, Vol. 54, (2016), 35-53.
16. A. Roine, et al., HSC Chemistry 6.0, in Chemical reaction and equilibrium software with extensive thermochemical database and flowsheet simulation, *Outotec* 2006, Pori, Finland.